DNA AND CELL BIOLOGY
Volume 44, Number 11, 2025
© Mary Ann Liebert, Inc.
Pp. 581–587
DOI: 10.1177/10445498251381313

Nucleosome Linker Length and Distribution as Major Players in Epigenetic Regulation: Insights from Cryo-Electron Microscopy and Modeling of Retina Cell Maturation

Tamar Schlick[1] and Sergei Grigoryev[2]

We summarize recent findings on the conformational differences of chromatin fibers in immature versus mature retina cells due to different nucleosome linker length values and distributions, as revealed by cryo-electron microscopy and modeling studies, emphasizing implications to chromatin organization and epigenetic regulation broadly.

Keywords: retina cells, linker DNA length, cryo-EM, mesoscale modeling, chromatin, epigenetic regulation

Introduction

The epigenetic regulation of human health and disease progression through chromatin conformational changes has been an important second code explored in recent years, in addition to the genetic code. Indeed, how cellular factors such as proteins, noncoding RNAs, and a variety of post-translational modifications influence the structure of the nucleosome-studded DNA chain in eukaryotes has been a fascinating area of biophysics with important implications to human development and health (Alberts et al., 2022; Willbanks et al., 2021; Mohanta et al., 2021; Baylin and Jones, 2011; Hendrich and Bickmore, 2001; Schlick et al., 2012).

Many textbooks depict the chromatin fiber as a regular chain with nucleosomes spaced with a fixed nucleosome repeat length and ordered helical folding (Alberts et al., 2022). In part, this view was supported by early structural studies based on X-ray crystallography and cryo-electron microscopy (cryo-EM) with single particle reconstruction that employed artificial nucleosome arrays with regular nucleosome linkers (e.g., Garcia-Saez et al., 2018; Li et al., 2024; Schalch et al., 2005; Song et al., 2014). In these approaches, all identical structural domains generate a near-atomic resolution signal, while dissimilarities generate noise that cannot be characterized structurally.

In recent years, the nucleosome positioning along the chromatin fiber, which defines internucleosome linker lengths (including nucleosome-free regions), has been a rich subject on its own right (Segal et al., 2006; Tilgner et al., 2009). Moreover, its relation to chromatin organization has been eagerly pursued. In chromatin fibers and genes, linker-DNA values adopt a large range that depends intimately on the cell type, organism, and cell state. Linker lengths also change in association with genetic disease; for example, Huntington's disease patients have nucleosomal and linker DNA with abnormal CAG repeats.

In the late 1970s, a variety of experiments quantified linker lengths across organisms, suggesting intriguing "phasing" patterns, related to the helical repeat of the DNA. For example, $10n$ and $10n + 5$ values where n is an integer were common. These preferred values affect chromatin organization in space because of a special relation to the periodicity of the B-DNA helix: for $10n$ linkers, nucleosome i and $i + 1$ would stack in a "phased" manner above one another, whereas nucleosomes in a regular $10n + 5$ fiber may not. Many experimental and modeling studies have explored these interesting findings, demonstrating different structural and hydrodynamic features of associated nucleosome arrays (recently reviewed in Li et al., 2025).

How are these irregularly spaced nucleosomes *in vivo* organized? In contrast to the artificial nucleosome arrays, no regular fibers have been observed in most eukaryotic cells by either super-resolution fluorescence microscopy (Nozaki et al., 2017; Ricci et al., 2015) or electron microscopy (Cai et al., 2018; Eltsov et al., 2008; Fussner et al., 2011; Ou et al., 2017).

Instead, real chromatin across many species reveals more irregular spacing that gives rise to signature conformational landscapes captured by modern chromosome experiments that characterize the frequency of contacts between genomic loci within the folded chromatin fiber. Both short and long linkers exist within the same nucleosome chain (Beel et al.,

[1]Department of Chemistry and Courant Institute of Mathematical Sciences, and Simons Center for Computational Physical Chemistry, New York University; and NYU-ECNU Center for Computational Chemistry, NYU Shanghai, Shanghai, China.
[2]Department of Molecular and Precision Medicine, Penn State University College of Medicine, Hershey, Pennsylvania, United States.

2021; Boltengagen et al., 2024; Jentink et al., 2023); thus, while a regular nucleosome spacing can certainly lead to special conformational patterns as found in $10n$ or $10n + 5$ linker values of regular chromatin arrays, the irregular nucleosome spacing encountered in practice, along with anchoring proteins *in vivo*, is a different story. This heterogeneity, in fact, leads to the interesting loop and stripe patterns we see in Hi-C maps today (Rao et al., 2017). For example, in the *GATA-4* gene, we found that hierarchical looping (stacked hairpins in 3D space) (Grigoryev et al., 2016) leads to folding over the transcription start site (Bascom et al., 2016). This emphasizes the structure/function connection of the nucleosomal positioning code.

As demonstrated in early modeling work (Bascom et al., 2017), regular linkers generate a limited pattern of internucleosome interactions (off-diagonal parts in internucleosome contact matrices), while irregular patterns for linker lengths yield self-folding interactions such as hairpins and hierarchical loops characterized by a rich variety of patterns within the off-diagonal elements (Bascom et al., 2016, 2017).

Nature exploits the profound impact of linker length on chromatin spatial organization in many regulatory processes. For example, in mouse development, nucleosome occupancy rises during differentiation. As mouse embryonic stem cells develop into neural progenitor cells, MNase-sequencing data, nanoscopic visualization, and mesoscale modeling reveal a concomitant transition of fiber compaction (Gómez-Garcia et al., 2021; Portillo-Ledesma et al., 2021); in particular, nucleosome clutch arrangements change from many groups of small nucleosomes to fewer groups with a larger number of nucleosomes per clutch.

Another recently explored pattern concerns chromatin reorganization in the process of retina rod cell maturation (Kable et al., 2025). Although the shape of the nucleosome distribution plot is similar, immature retina cells have a shifted distribution by about 10–15 bp shorter linkers, some with very short values that correspond to unwrapping of the DNA around the nucleosome core. The details of these contrasting fibers were analyzed by a collaboration between experimental and modeling teams (Kable et al., 2025).

In brief, the differences in linker length values and distributions give rise to a ladder-like chromatin fiber topology in immature retina cells rather than typical zigzag arrangements where nucleosomes i and $i \pm 2$ are in close contact along the chain (Bascom et al., 2016; Bascom and Schlick, 2018). The larger values in mature retina cells, with both shorter and longer values and larger average values, lead not only to a tight zigzag chromatin arrangement but also an interconnected network between nucleosomes sealed by stems—zipper-like arrangements between a nucleosome's two linkers and its associated linker histones (LHs). We elaborate upon these studies below and discuss their significance at large to epigenetic regulation of gene activity.

Experimental Characterization of Chromatin Fibers During Retina Cell Maturation

The eye retina belongs to the central nervous system and is an important model for studies related to epigenetic mechanisms of neuronal differentiation (Aldiri et al., 2017; Popova et al., 2013; Solovei et al., 2009). Malfunction of this process can lead to blindness (Jorstad et al., 2017; Popova et al., 2021) and other neurodegenerative disorders (Alkhammash and Alotaibi, 2025).

The majority of cells in the mouse retina (about 85%) is represented by rod photoreceptors (Aldiri et al., 2017). This cell type undergoes prominent changes in chromatin organization during cell maturation. While immature retina rod cells have relatively open euchromatin (Fig. 1A), accessible

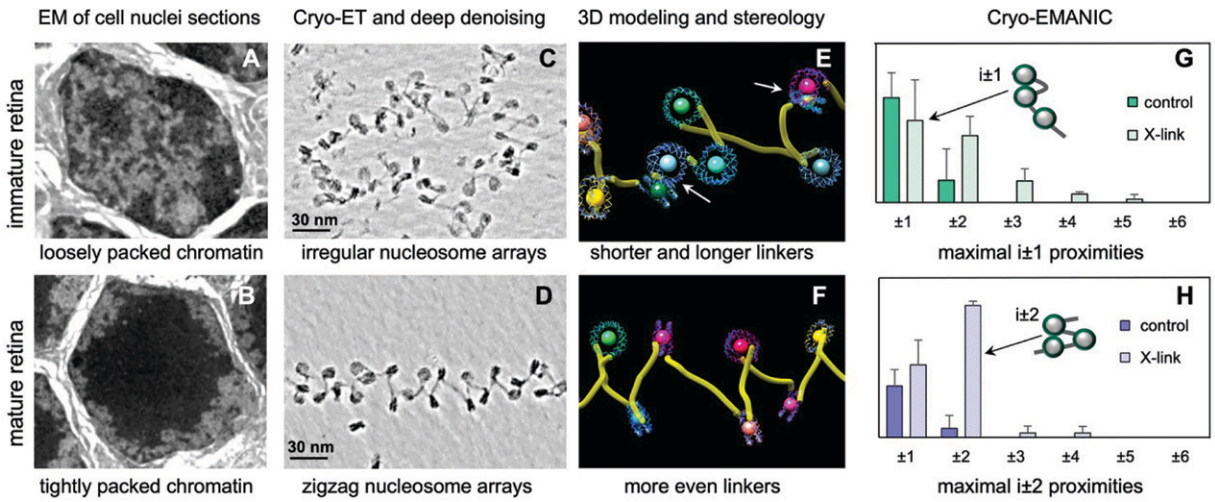


FIG. 1. Chromatin structural transitions during retina rod cell maturation: 3D analysis by cryo-ET and stereological modeling. **(A, B)**: Transmission electron microscopy of cell sections from immature **(A)** and mature **(B)** mouse rod photoreceptors obtained at postnatal days 1 **(A)** and 56 **(B)**. **(C, D)** Chromatin isolated from immature **(C)** and mature **(D)** retina rod cells visualized by cryo-ET in 3D aided by deep-learning de-noising. **(E, F)**: Stereological models derived from cryo-ET images aided by nucleosome core X-ray crystal structure fitting and linker DNA tracing. White arrows show pairs of closely overlapped nucleosomes without linkers. **(G, H)**: EMANIC analysis of nearest-neighbor nucleosome interactions captured by *in situ* chromatin crosslinking in immature **(G)** and mature **(H)** with subsequent isolation and cryo-ET imaging. Panels A, B: modified from Popova et al. (2013); panels C–H: modified from Kable et al. (2025). EMANIC, EM-assisted nucleosome interaction capture.

for transcription, the mature rod cell nuclei are associated with silent genes, which remain within the condensed chromatin portion, or heterochromatin around the nuclear periphery (Fig. 1B). When young mice grow older, their rod cell nucleus undergoes a striking process called *chromatin inversion*: the condensed chromatin relocates to the center of the nucleus while the active euchromatin moves to the nuclear periphery (Popova et al., 2013; Solovei et al., 2009). This chromatin reorganization phenomenon allows researchers to study the well-segregated genome compartments specific for euchromatin and heterochromatin.

To characterize the chromatin structural transitions occurring during retina maturation at the nucleosomal level, we turned to cryo-EM tomography (Cryo-ET) to generate 3D images of individual particles embedded in vitrified ice from a series of tilted images (Palao et al., 2024). Currently, the resolution of cryo-ET (about 10 Å) is less than that of the single-particle cryo-EM but it allows analysis of individual nucleosome arrays with subnucleosomal resolution. The sharp images of the DNA coiled in the nucleosome (Fig. 1C, D) make possible stereological measurements to deduce internucleosome distances and plane angles in the open and condensed forms, as well as the length of DNA wrapped around each nucleosome core and between nucleosomes (Jentink et al., 2023).

With cryo-ET, we observed a striking difference between the chromatin organization in the immature, postnatal day 1 (PN1) and mature, postnatal day 56 (PN56) rod cell chromatin: immature retina featured a much stronger heterogeneity of the nucleosome linker length (Fig. 1C) than mature cells, where linkers become more even and tend to fold into a typical zigzag array (Fig. 1D). Stereological modeling and measurements of the individual linker length in immature (Fig. 1E) versus mature (Fig. 1F) rod cells revealed not only a significant increase during maturation but also a population of very close juxtaposed nucleosomes with negative linker length in immature cells (arrows on Fig. 1E). This type of linker originates from partially overlapping nucleosome core in which supercoiled DNA from one core particle merges with that of the next nucleosome (Fig. 1F). Such overlapping nucleosomes have been associated with transcription start sites; here, they make a substantial fraction of total cellular chromatin: 10.7% of all nucleosome linker lengths in immature retina have negative values compared with just 3.2% in mature retina.

How do these striking differences in nucleosome linker lengths translate to chromatin folding for immature versus mature retina cells? By combining cryo-ET with our previously developed EM-assisted nucleosome interaction capture (EMANIC) cross-linking approach (Grigoryev et al., 2016; Popova et al., 2009), we capture nucleosome interactions in the cell nuclei by formaldehyde cross-linking. When followed by chromatin isolation and scoring contacts between nearest-neighbor nucleosomes and cryo-ET, the internucleosome interactions can be characterized: $i/i \pm k$ where i represents a nucleosome index and $k = 1, 2, 3, \ldots$. EMANIC analysis shows that the level of the $i \pm 2$ interactions is high for the mature retina (Fig. 1H), while $i \pm 1$ contacts are high for immature cells (Fig. 1G). Immature cells also exhibit a notable increase of $i \pm 3$ and $i \pm 4$ interactions.

Importantly, the contact distribution in mature retina (Fig. 1H) strongly resembles that in the regular reconstituted chromatin folded into the two-start zigzag (Grigoryev et al., 2016). Thus, the increased chromatin condensation during retina maturation appears to be mediated by increasing nucleosome linker lengths and the associated chromatin folding into the two-start zigzag, without forming regular 30 nm fibers, as assumed historically.

Modeling Analysis of Chromatin Fibers in Retina Cell Maturation

In tandem, our modeling team constructed chromatin fibers with linker lengths taken directly from the experimental distributions and applied our chromatin mesoscale model (reviewed in Bascom and Schlick, 2017; Portillo-Ledesma and Schlick, 2020; Portillo-Ledesma et al., 2023; Portillo-Ledesma and Schlick, 2024) to simulate chromatin fibers typical of the PN1 (immature) and PN56 (mature) stages. The chromatin mesoscale model combines coarse-grained representations of nucleosome cores, histone tails, linker DNA, and linker histones (LHs) within chromatin fiber arrays (see Luque et al., 2014; Portillo-Ledesma et al., 2022).

For each system, PN1 and PN56, 23-nucleosome arrays were simulated similar to the experimental systems. Because the mesoscale model is coarse-grained, linker values closest to the experimental values were set. This effectively assigned linker values from 0 to 115 bp (0, 17.65, 26.47, 35.29, 44.12, 52.94, 61.76, 70.59, 79.41, and 114.71 bp). Both the PN1 and PN56 fibers were simulated with saturated LH of one molecule per nucleosome based on experimental measurements for mouse retina. The salt milieu was set to both 5 and 150 mM NaCl concentration, with and without the addition of 1 mM Mg^{2+}, the latter introduced implicitly (Grigoryev et al., 2009).

From a statistical ensemble of equilibrium Monte Carlo sampling, we analyzed representative PN1 and PN56 conformations, calculating packing ratios (the number of nucleosomes in 11 nm of fiber), internucleosome interactions, and tail interactions. We also generated fan plots from single trajectories to visualize linker/LH interactions along each nucleosomal plane, and the linker DNA cumulative and average positional distribution. This allowed us to assess quantitatively the degree of stem formation by measuring average distances associated with the two linkers from the same nucleosome expressing a stem.

The representative conformations in Figure 2 show distinct folding patterns. While PN1 fibers appear in a ladder-like arrangement dictated by short linker spacing, somewhat tighter at high salt, the PN56 conformations show an open chain at low salt and very tight self-folding patterns at high salt with significantly higher packing ratio.

The stem analysis in Figure 3 clarifies the mechanism: the short linkers in PN1 make it impossible to form optimal stems, because the LH protein has an end-to-end distance much larger than the linker value. And an occasional long linker in PN1 leads at best to an asymmetrical arrangement with one linker rather than both. In contrast, PN56 fibers with longer linkers form a variety of stem arrangements, even when exiting and entering linker lengths differ substantially.

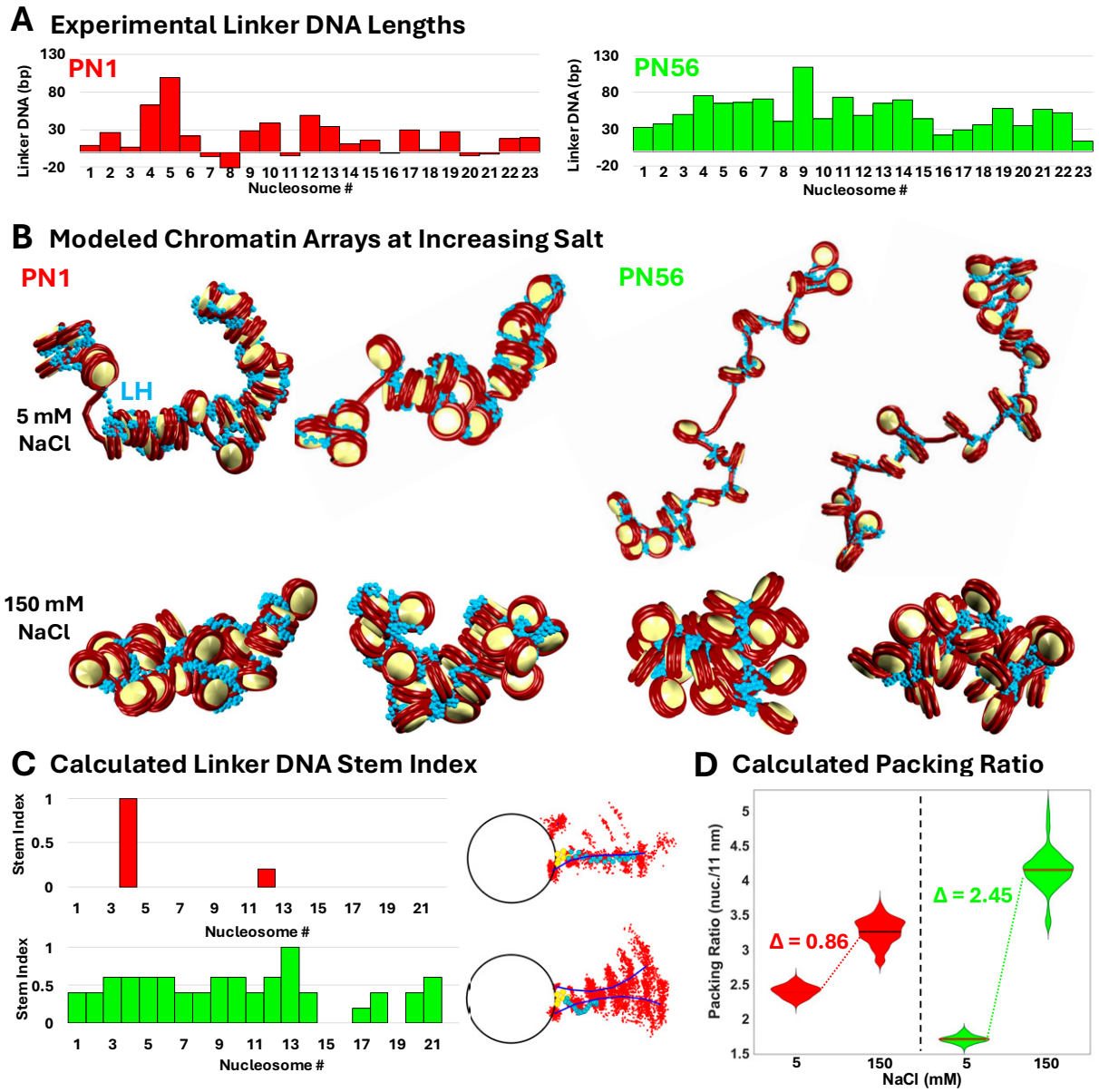


FIG. 2. Modeling findings on key differences between immature (PN1) versus mature (PN56) retina cells. Shown are the linker length values **(A)**, representative conformations **(B)**, stem strength assessment based on linker/linker contact distances **(C)**, and compaction measurements **(D)**.

Epigenetic Regulation Implications

Our combined studies reveal a global trend in chromatin reorganization accompanying retina rod cell maturation. In immature retina, short nucleosome linkers make the nucleosome arrays relatively open; as retina cells mature, linker length increases, and the chromatin becomes increasingly condensed.

The mechanism for this condensation is linker DNA stem formation (Fig. 3), which mediates zigzag chromatin folding.

Such a linker-length-driven epigenetic mechanism may be more generally associated with higher-order chromatin folding in many cell states and conditions. The facile tunability of this stem-driven compaction mechanism makes it applicable to many condensation phenomena in the cell, where salt, binding proteins, and chemical modifications can easily shift conformational states and hence DNA transcription.

The epigenetic regulation of genomes is tightly orchestrated by a host of factors: post-translational histone modifications, enzymes that impose these histone modifications, and nonhistone proteins. In a general model of epigenetic regulation called the *histone code* (Jenuwein and Allis, 2001), the modified histones are established by histone-modifying enzymes (e.g., histone acetyltransferases and methyltransferases) called the *histone code writers* and attract architectural nonhistone proteins called *histone code readers* (e.g., heterochromatin protein 1 or HP1), which impose chromatin condensation on heterochromatin.

Remarkably, in a number of mature tissue cell types (Gilbert et al., 2003; Istomina et al., 2003) including retina photoreceptors (Popova et al., 2013), HP1 is dramatically reduced and cannot fulfill its chromatin condensation

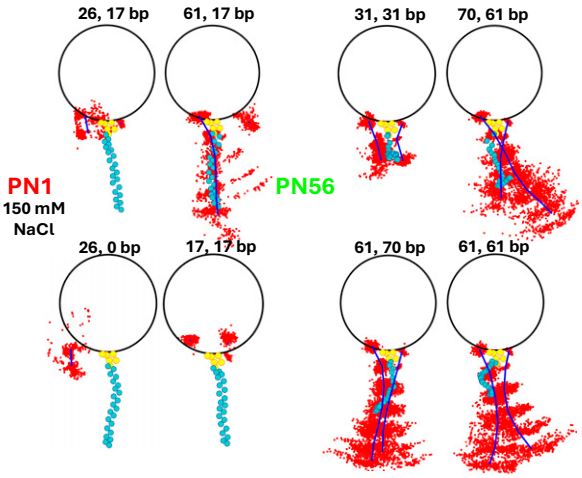


FIG. 3. Modeling findings on stem formation differences between immature (PN1) versus mature (PN56) retina cells. For each cell type, the fan plots present side views of nucleosome planes with entering and exiting linkers (*red*, with lengths in bp given) binding to linker histones (*turquoise*). Mature retina linker lengths make possible much stronger stems, even with the two linkers have disparate values. The short linker of immature retina cells make stem formation very difficult.

function. Instead, mature mouse retina chromatin is likely to be condensed by LH H1. Evidence shows that H1 increases during retina maturation (Popova et al., 2013), and that its binding is promoted by longer nucleosome linkers (Dombrowski et al., 2022). Extensive modeling has revealed the condensation mechanism where linkers similar to the size of the LH protein when stretched lead to optimal stems (Collepardo-Guevara and Schlick, 2012, 2014; Luque et al., 2014, 2016; Portillo-Ledesma, Wagley and Schlick, 2022).

The mechanism of epigenetic regulation by variable nucleosome linker lengths that we have proposed requires a better understanding of chromatin positioning factors responsible for such nucleosome assignment during retina maturation, or during euchromatin to heterochromatin transitions. Nucleosome spacing in eukaryotic cells is established and supported by ATP-dependent chromatin remodeling complexes (Narlikar et al., 2013). Certain chromatin remodelers such as the mating type switching and sucrose non-fermenting (SWI/SNF) family move individual nucleosomes to generate open nucleosome-free regions and closely overlapping nucleosomes (Ulyanova and Schnitzler, 2005). Other chromatin remodelers such as imitation switch (ISW) work as molecular rulers cooperatively to generate more regular beads-on-a-string arrays (Bomber et al., 2023; Vizjak et al., 2024).

Intriguingly, SWI/SNF homolog BRG1 (*Smarca4*) mediates cell integrity in early retina progenitors (Holdhof et al., 2021), while ISWI (*SmarcA5*) is essential for photoreceptor maintenance (Kuzelova et al., 2023). Perhaps, in addition to histone code readers, writers, and erasers, the epigenetic mechanisms regulating euchromatin and heterochromatin spreading involve a balance between nucleosome mobilizers (such as SWI/SNF) and stabilizers (such as ISWI and LH H1).

As we have demonstrated, deciphering nucleosome and chromatin folding by cryo-ET and multiscale modeling opens a new avenue for understanding epigenetic mechanisms driving cell differentiation and discriminating between normal cell function and disease states. Besides revealing this compaction mechanism and the crucial role that linker length distributions have on retina cell development, our study underscores the importance of experimental/physics-based modeling collaborations to decipher biological mechanisms, a goal not easily achieved by AI analysis alone.

Authors' Contributions

Both authors wrote and edited the manuscript.

Acknowledgment

T.S. acknowledges support from the National Science Foundation Award 2337391, National Institutes of Health, National Institute for General Medical Sciences Award R35-GM12256, and the Simons Foundation through the NYU Simons Center for Computational Physical Chemistry. S.G. acknowledges support from the National Science Foundation Award 191194 and National Institutes of Health R21 DA056343.

Author Disclosure Statement

No interests to disclose.

Funding Information

No funding was received for this article.

References

Alberts B, Heald R, Johnson A, et al. (2022), Molecular Biology of the Cell, seventh edn, W. W. Norton & Company, New York, NY.

Aldiri I, Xu B, Wang L, et al.; St. Jude Children's Research Hospital—Washington University Pediatric Cancer Genome Project. 'The dynamic epigenetic landscape of the retina during development, reprogramming, and Tumorigenesis'. Neuron 2017;94(3):550–568.e10.

Alkhammash A, Alotaibi G. 'Epigenetic reprogramming as a therapeutic strategy for neurodegenerative diseases: A complex and novel Approach'. Eur J Pharmacol 2025;1002:177853.

Bascom G, Schlick T. (2017), Mesoscale modeling of chromatin fibers, *in* C Lavelle & J.-M Victor., eds, 'Nuclear Architecture and Dynamics', Academic Press, Elsevier, chapter 4, pp. 123–148.

Bascom G, Schlick T. 'Chromatin fiber folding directed by cooperative histone tail acetylation and linker histone Binding'. Biophys J 2018;114(10):2376–2385.

Bascom G, Kim T, Schlick T. 'Kilobase pair chromatin fiber contacts promoted by living-system-like DNA linker length distributions and nucleosome Depletion'. J Phys Chem B 2017;121(15):3882–3894.

Bascom G, Sanbonmatsu K, Schlick T. 'Mesoscale modeling reveals hierarchical looping of chromatin near gene regulatory Elements'. J Phys Chem B 2016;120(33):8642–8653.

Baylin SB, Jones PA. 'A decade of exploring the cancer epigenome—biological and translational Implications'. Nat Rev Cancer 2011;11(10):726–734.

Beel AJ, Azubel M, Mattei PJ, et al. 'Structure of mitotic Chromosomes'. Mol Cell 2021;81(21):4369–4376.e3.

Boltengagen M, Verhagen D, Wolff MR, et al. 'A single fiber view of the nucleosome organization in eukaryotic Chromatin'. Nuc. Acids Res 2024;52(1):166–185.

Bomber ML, Wang J, Liu Q, et al. 'Human smarca5 is continuously required to maintain nucleosome Spacing'. Mol Cell 2023;83(4):507–522.e6.

Cai S, Chen C, Tan ZY, et al. 'Cryo-ET reveals the macromolecular reorganization of S. pombe mitotic chromosomes in Vivo'. Proc Natl Acad Sci U S A 2018;115(43):10977–10982.

Collepardo-Guevara R, Schlick T. 'Crucial role of dynamic linker histone binding for DNA accessibility and gene regulation revealed by mesoscale modeling of Oligonucleosomes'. Nucleic Acids Res 2012;40(18):8803–8817.

Collepardo-Guevara R, Schlick T. 'Chromatin fiber polymorphism triggered by variations of DNA linker Lengths'. Proc Natl Acad Sci U S A 2014;111(22):8061–8066.

Dombrowski M, Engeholm M, Dienemann C, et al. 'Histone H1 binding to nucleosome arrays depends on linker DNA length and Trajectory'. Nat Struct Mol Biol 2022;29(5):493–501.

Eltsov M, Maclellan KM, Maeshima K, et al. 'Analysis of cryo-electron microscopy images does not support the existence of 30-nm chromatin fibers in mitotic chromosomes in Situ'. Proc Natl Acad Sci U S A 2008;105(50):19732–19737.

Fussner E, Ching RW, Bazett-Jones DP. 'Living without 30nm chromatin Fibers'. Trends Biochem Sci 2011;36(1):1–6.

Gómez-Garcia PA, Portillo-Ledesma S, Neguembor MV, et al. 'Mesoscale modeling and single-nucleosome tracking reveal remodeling of clutch folding and dynamics in stem cell Differentiation'. Cell Rep 2021;34(2):108614.

Garcia-Saez I, Menoni H, Boopathi R, et al. 'Structure of an H1-bound 6-nucleosome array reveals an untwisted two-start chromatin fiber Conformation'. Mol Cell 2018;72(5):902–915.e7.

Gilbert N, Boyle S, Sutherland H, et al. 'Formation of facultative heterochromatin in the absence of HP1'. Embo J 2003; 22(20):5540–5550.

Grigoryev SA, Arya G, Correll S, et al. 'Evidence for heteromorphic chromatin fibers from analysis of nucleosome Interactions'. Proc Natl Acad Sci U S A 2009;106(32):13317–13322.

Grigoryev S, Bascom G, Schubert M, et al. 'Hierarchical looping of zigzag nucleosome chains in metaphase Chromosomes'. Proc Natl Acad Sci U S A 2016;113(5):1238–1243.

Hendrich B, Bickmore W. 'Human diseases with underlying defects in chromatin structure and Modification'. Hum Mol Genet 2001;10(20):2233–2242.

Holdhof D, Schoof M, Al-Kershi S, et al. 'Brahma-related gene 1 has time-specific roles during brain and eye Development'. Development 2021;148(10):dev196147.

Istomina N, Shushanov S, Springhetti E, et al. 'Insulation of the chicken beta-globin chromosomal domain from a chromatin-condensing protein, ment. Mol Cell Biol 2003; 23(18):6455–6468.

Jentink N, Purnell C, Kable B, et al. 'Cryoelectron tomography reveals the multiplex anatomy of condensed native chromatin and its unfolding by histone Citrullination'. Mol Cell 2023; 83(18):3236–3252.e7.

Jenuwein T, Allis CD. 'Translating the histone Code'. Science 2001;293(5532):1074–1080.

Jorstad NL, Wilken MS, Grimes WN, et al. 'Stimulation of functional neuronal regeneration from muller glia in adult Mice'. Nature 2017;548(7665):103–107.

Kable B, Portillo-Ledesma S, Popova E, et al. 'Compromised 2-start zigzag chromatin folding in immature mouse retina cells driven by irregularly spaced nucleosomes with short DNA Linkers'. Nucl. Acids Res 2025;53(10):gkaf457.

Kuzelova A, Dupacova N, Antosova B, et al. 'Chromatin remodeling enzyme Snf2h is essential for retinal cell proliferation and photoreceptor Maintenance'. Cells 2023;12(7):1035.

Li W, Hu J, Song F, et al. 'Structural basis for linker histone H5-nucleosome binding and chromatin fiber Compaction'. Cell Res 2024;34(10):707–724.

Li Z, Portillo-Ledesma S, Schlick T. 'Chromatin higher-order folding as influenced by preferred linker DNA values'. Curr Opin Struct Biol 2025;95:103154. Special issue on Protein Nucleic-Acid Interactions. S Ahmad and E Laine., Gest Eds; doi: 10.1016/j.sbi.2025.103154

Luque A, Collepardo-Guevara R, Grigoryev S, et al. 'Dynamic condensation of linker histone C-terminal domain regulates chromatin Structure'. Nucleic Acids Res 2014;42(12): 7553–7560.

Luque A, Ozer G, Schlick T. 'Correlation among DNA linker length, linker histone concentration, and histone tails in Chromatin'. Biophys J 2016;110(11):2309–2319.

Mohanta TK, Mishra AK, Al-Harrasi A. 'The 3D genome: From structure to Function'. Int J Mol Sci 2021;22(21): 11585.

Narlikar GJ, Sundaramoorthy R, Owen-Hughes T. 'Mechanisms and functions of ATP-dependent chromatin-remodeling Enzymes'. Cell 2013;154(3):490–503.

Nozaki T, Imai R, Tanbo M, et al. 'Dynamic organization of chromatin domains revealed by super-resolution live-cell Imaging'. Mol Cell 2017;67(2):282–293.e7.

Ou HD, Phan S, Deerinck TJ, et al. 'ChromEMT: Visualizing 3D chromatin structure and compaction in interphase and mitotic Cells'. Science 2017;357(6349):eaag0025.

Palao L, , Third, Murakami K, Chang YW. 'Combining per-particle cryo-ET and cryo-EM single particle analysis to elucidate heterogeneous DNA-protein Organization'. Curr Opin Struct Biol 2024;84:102765.

Popova EY, Grigoryev SA, Fan Y, et al. 'Developmentally regulated linker histone H1c promotes heterochromatin condensation and mediates structural integrity of rod photoreceptors in mouse Retina'. J Biol Chem 2013;288(24):17895–17907.

Popova EY, Imamura Kawasawa Y, Zhang SS, et al. 'Inhibition of epigenetic modifiers lsd1 and hdac1 blocks rod photoreceptor death in mouse models of retinitis Pigmentosa'. J Neurosci 2021;41(31):6775–6792.

Popova E, Krauss S, Short S, et al. 'Chromatin condensation in terminally differentiating mouse erythroblasts does not involve special architectural proteins but depends on histone Deacetylation'. Chromosome Res 2009;17(1):47–64.

Portillo-Ledesma S, Schlick T. 'Bridging chromatin structure and function over a range of experimental spatial and temporal scales by molecular Modeling'. WIREs Comp. Mol. Sci 2020;10(2):e1434.

Portillo-Ledesma S, Schlick T. 'Regulation of chromatin architecture by protein binding: Insights from molecular Modeling'. Biophys Rev 2024;16(3):331–343. Special Ascona meeting issue, Multiscale Simulations of DNA from Electrons to Nucleosome, W. Olson et al., Eds.

Portillo-Ledesma S, Li Z, Schlick T. 'Genome modeling: From chromatin fibers to Genes'. Curr Opin Struct Biol 2023;78: 102506. Special issue on Theory and Simulation/Computational Methods, T. Haliloglu and G. Voth, Eds.

Portillo-Ledesma S, Tsao LH, Wagley M, et al. 'Nucleosome clutches are regulated by chromatin internal Parameters'. J Mol Biol 2021;433(6):166701.

Portillo-Ledesma S, Wagley M, Schlick T. 'Chromatin transitions triggered by LH density as epigenetic modulators of the Genome'. Nucl. Acids Res 2022;50(18):10328–10342.

Rao SSP, Huang S-C, Hilaire BGS, et al. 'Cohesin loss eliminates all loop domains, leading to links among superenhancers and downregulation of nearby Genes'. Cell 2017; 171(2):305–320.e24.

Ricci MA, Manzo C, García-Parajo MF, et al. 'Chromatin fibers are formed by heterogeneous groups of nucleosomes In 'vivo. Cell 2015;160(6):1145–1158.

Schalch T, Duda S, Sargent DF, et al. 'X-ray structure of a tetranucleosome and its implications for the chromatin Fibre'. Nature 2005;436(7047):138–141.

Schlick T, Hayes J, Grigoryev SA. 'Toward convergence of experimental studies and theoretical modeling of the chromatin Fiber'. J Biol Chem 2012;287(8):5183–5191.

Segal E, Fondufe-Mittendorf Y, Chen L, et al. 'A genomic code for nucleosome Positioning'. Nature 2006;442(7104):772–778.

Solovei I, Kreysing M, Lanctot C, et al. 'Nuclear architecture of rod photoreceptor cells adapts to vision in mammalian Evolution'. Cell 2009;137(2):356–368.

Song F, Chen P, Sun D, et al. 'Cryo-EM study of the chromatin fiber reveals a double helix twisted by tetranucleosomal Units'. Science 2014;344(6182):376–380.

Tilgner H, Nikolaou C, Althammer S, et al. 'Nucleosome positioning as a determinant of exon Recognition'. Nat Struct Mol Biol 2009;16(9):996–1001.

Ulyanova NP, Schnitzler GR. 'Human swi/snf generates abundant, structurally altered dinucleosomes on polynucleosomal Templates'. Mol Cell Biol 2005;25(24):11156–11170.

Vizjak P, Kamp D, Hepp N, et al. 'Iswi catalyzes nucleosome sliding in condensed nucleosome Arrays'. Nat Struct Mol Biol 2024;31(9):1331–1340.

Willbanks A, Wood S, Cheng JX. 'RNA epigenetics: Fine-tuning chromatin plasticity and transcriptional regulation, and the implications in human Diseases'. Genes (Basel) 2021; 12(5):627.

Address correspondence to:
Tamar Schlick, PhD
Silver Center
Suite 1021
100 Washington Square East
Department of Chemistry
New York University
New York, NY 10003
United States

E-mail: schlick@nyu.edu

Sergei Grigoryev, PhD
Department of Molecular and Precision Medicine
Penn State University College of Medicine
500 University Drive
Hershey, PA 17033
United States

E-mail: sag17@psu.edu

Received for publication August 4, 2025; received in revised from August 4, 2025; accepted August 6, 2025.